nature ecology & evolution

Analysis

https://doi.org/10.1038/s41559-025-02961-8

Microbial growth rate is a stronger predictor of soil organic carbon than carbon use efficiency

Received: 25 June 2025

Accepted: 11 December 2025

Published online: 06 February 2026

Check for updates

Xianjin He[1,12], Gaëlle Marmasse[1,12], Junxi Hu[2] ✉, Rebecca M. Varney[3,4], Stefano Manzoni[3], Philippe Ciais[1], Ying-Ping Wang[5,6], Yongxing Cui[7], Edith Bai[8,9], Rose Z. Abramoff[10], Elsa Abs[1], Erik Schwarz[3], Haicheng Zhang[11] & Daniel S. Goll[1] ✉

The extent to which microbial processes control soil organic carbon (SOC) dynamics remains uncertain. Carbon use efficiency (CUE), that is, the fraction of assimilated carbon allocated to growth, has been used as a key parameter but its relationship with SOC reflects carbon partitioning rather than the absolute magnitude of microbial fluxes. The microbial growth rate could provide a more mechanistic link to SOC accumulation because it quantifies biomass production and reflects necromass formation. Here we combine a global ^{18}O–H_2O dataset (n = 268 paired observations) with outputs from four land surface models to test whether growth rate predicts SOC more strongly than CUE. In the incubation experiments, growth rates are more closely associated with SOC than CUE, although soil properties and climate explain equal or greater variance. Models reproduce the stronger role of growth rate over CUE but tend to underestimate the abiotic controls. The models also emphasize CUE as the main predictor of the SOC-to-net primary production ratio, in contrast to observations, which indicates the soil's capacity to retain plant carbon inputs. Together, these findings identify the microbial growth rate as a diagnostic that can help bridge models with empirical data and guide a more balanced representation of microbial and mineral controls in SOC projections.

A key principle in soil carbon research is that carbon fluxes, rather than static pool sizes, are more directly linked to ecosystem function[1,2]. Microorganisms exemplify this principle, where although microbial biomass typically accounts for less than 5% of total soil organic carbon (SOC)[3], microbial residues (necromass) can contribute over 50% of SOC[4,5]. This reflects their disproportionate and lasting contribution to long-term soil carbon sequestration. This enduring contribution arises from rapid cycling of microbial biomass, which regulates the fluxes of microbial carbon uptake, respiration, growth and death[6]. Therefore, microbial communities act as a biological pump actively shaping SOC dynamics[7], complementing the mineral pump that stabilizes organic matter through mineral interactions[8].

However, in efforts to quantify microbial control over SOC dynamics, recent studies have focused on microbial carbon use efficiency (CUE), that is, the proportion of assimilated carbon allocated to growth, as a key parameter linking microbial activity to SOC. Several modelling studies suggest that CUE strongly affects SOC stocks[9–11], with Tao et al.[12] reporting that global variations in CUE exert a greater influence on SOC than any other model parameter. However, this claim remains contested. Subsequent work has highlighted methodological concerns such as equifinality in inverse modelling[13] and the omission of

A full list of affiliations appears at the end of the paper. ✉e-mail: junxihu@sicau.edu.cn; dsgoll123@gmail.com

https://doi.org/10.1038/s41559-025-02961-8

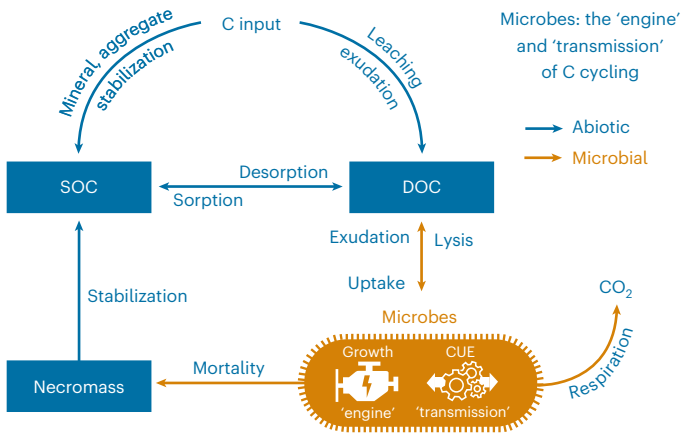

Fig. 1 | Conceptual model of microbial regulation of soil carbon cycling. This diagram uses a mechanical metaphor in which microbial growth rate functions as the 'engine' driving carbon fluxes, while CUE serves as the 'transmission' modulating the partitioning of carbon between biomass production and CO_2 release. Plant carbon inputs can contribute to SOC through mineral and aggregate stabilization, or enter the dissolved organic carbon (DOC) pool via leaching of soluble litter and root exudation. Exchanges between SOC and DOC occur through sorption and desorption. Microbes assimilate DOC and either respire carbon or allocate it to growth. Microbial exudation and lysis release dissolved organic matter back to the DOC pool, whereas stabilized microbial necromass contributes to SOC. The orange arrows represent microbially mediated cycling, while the blue arrows indicate physicochemical processes, including plant-derived inputs. For clarity, all arrows are drawn with equal thickness to represent pathways rather than quantified flux magnitudes.

key physicochemical stabilization processes[14], while empirical studies found inconsistent SOC–CUE relationships[15–22]. More fundamentally, CUE is a ratio property; it describes carbon partitioning between growth and respiration but does not capture the absolute magnitude of microbial carbon fluxes. Consequently, a high CUE does not necessarily result in greater SOC accumulation. If microbial biomass turns over rapidly, assimilated carbon may be quickly respired or recycled, limiting its contribution to long-term storage[12,23]. Conversely, a low CUE does not necessarily limit SOC accumulation. When microbial processing is inefficient and decomposition rates are slow, organic carbon can still progressively accumulate over time depending on stabilization by mineral interactions[24,25]. These scenarios highlight that CUE captures only part of the microbial influence on SOC and that the variability of SOC ultimately reflects both microbial process rates and the strength of physicochemical stabilization.

Microbial growth rate, which quantifies the gross rate of biomass production, offers a more mechanistic and process-based metric linking carbon assimilation to microbial biomass cycling and necromass formation[26]. Accumulating evidence suggests that the growth rate may show a stronger association with SOC dynamics than CUE because the microbial growth rate reflects the production and cycling of microbial residues, which are key precursors to stable SOC[18]. Moreover, while both the microbial growth rate and CUE are ecologically meaningful properties, the growth rate is more plastic and responsive to environmental variation[11,27,28], whereas CUE is often more constrained across conditions[11,27–29].

In this study, we adopt an integrative framework, which is common in process-based models but less emphasized in experimental studies, in which microbial process rates such as uptake and growth, together with CUE, jointly regulate SOC dynamics. In this framework, microbial process rates act as the engine driving carbon fluxes, with CUE serving as the transmission that modulates their efficiency (Fig. 1). This highlights the microbial growth rate as the direct mechanistic link to SOC dynamics, with CUE operating as a secondary modulator[30,31].

In this study, we combine a global observational dataset derived from the ^{18}O–H_2O labelling method, a robust and widely used approach for quantifying microbial growth rates and CUE[32,33], with outputs from four land surface models (ORCHIDEE-CENTURY, ORCHIDEE-MIMICS, JULES-RothC and CABLE-CASA). We ask whether the microbial growth rate is a stronger predictor of observed spatial variation in SOC than CUE or abiotic factors underpinning the mineral pump of SOC stabilization. In addition, we introduce a diagnostic framework that connects microbial observations with model outputs, offering a clearer way to evaluate model performance and improve predictions of soil carbon change.

Results

Observed SOC is more strongly linked to microbial growth than to CUE but even more to abiotic factors

Using 268 paired observations obtained via the ^{18}O–H_2O labelling method across diverse ecosystems (Supplementary Fig. 1), we examined the relationships between SOC and microbial or ecosystem properties (Fig. 2). Bivariate regressions identified significant positive correlations between SOC and the microbial absolute growth rate (that is, microbial biomass production per unit soil mass per unit time; $R^2 = 0.371$, $P < 0.001$), microbial respiration rate ($R^2 = 0.269$, $P < 0.001$), microbial biomass ($R^2 = 0.285$, $P < 0.001$) and, to a much lesser extent, microbial CUE ($R^2 = 0.015$, $P = 0.046$). On the other hand, the microbial specific growth rate (that is, the microbial growth rate normalized to the microbial biomass; $R^2 < 0.001$, $P = 0.999$) and net primary production (NPP) (derived from MODIS; $R^2 < 0.001$, $P = 0.999$) showed no significant relationship with SOC. These results indicate that SOC covaries more strongly with microbial absolute growth and biomass than with CUE, specific growth rate or plant productivity.

Random forest regression confirmed these patterns: the microbial growth rate was a stronger predictor of SOC than CUE; however, the soil clay content and the mean annual temperature (MAT) explained comparable or even greater variation (Fig. 3a). Thus, while the growth rate provides a clearer microbial link to SOC than CUE, abiotic constraints remain equally or even more important.

The positive association between absolute microbial growth rate and SOC mainly reflected microbial biomass regulation by SOC availability: the absolute growth rate correlated with microbial biomass ($R^2 = 0.237$, $P < 0.001$), respiration ($R^2 = 0.381$, $P < 0.001$) and, to a lesser extent, specific growth rate ($R^2 = 0.219$, $P < 0.001$; Supplementary Fig. 2a). On the other hand, soil microbial CUE showed no significant relationship with microbial biomass ($R^2 = 0.015$, $P = 0.094$), a negative relationship with the microbial respiration rate ($R^2 = 0.245$, $P < 0.001$), a modest positive relationship with the specific microbial growth rate ($R^2 = 0.209$, $P < 0.001$) and a weak positive relationship with the absolute microbial growth rate ($R^2 = 0.119$, $P < 0.001$; Supplementary Fig. 2b). Together, these patterns indicate that the absolute microbial growth rate, or the associated respiration rate, captures SOC variation more consistently than microbial CUE, which is largely decoupled from both SOC and microbial biomass.

Because microbial growth rates were measured under controlled laboratory conditions, we examined their sensitivity to incubation temperature. Growth rates exhibited only weak temperature dependence, both in absolute terms ($R^2 = 0.02$, $P = 0.034$; Supplementary Fig. 3a) and when normalized by SOC to account for pool-size effects ($R^2 = 0.01$, $P = 0.142$; Supplementary Fig. 3b). These results indicate that the observed variation in microbial growth mainly reflects actual site differences rather than artefacts of incubation temperature.

Model simulations overemphasizes microbial traits relative to abiotic factors

We next tested whether four land surface models, that is, ORCHIDEE-CENTURY, ORCHIDEE-MIMICS, JULES-RothC and CABLE-CASA, reproduce the stronger SOC–growth link. Among them, only

https://doi.org/10.1038/s41559-025-02961-8

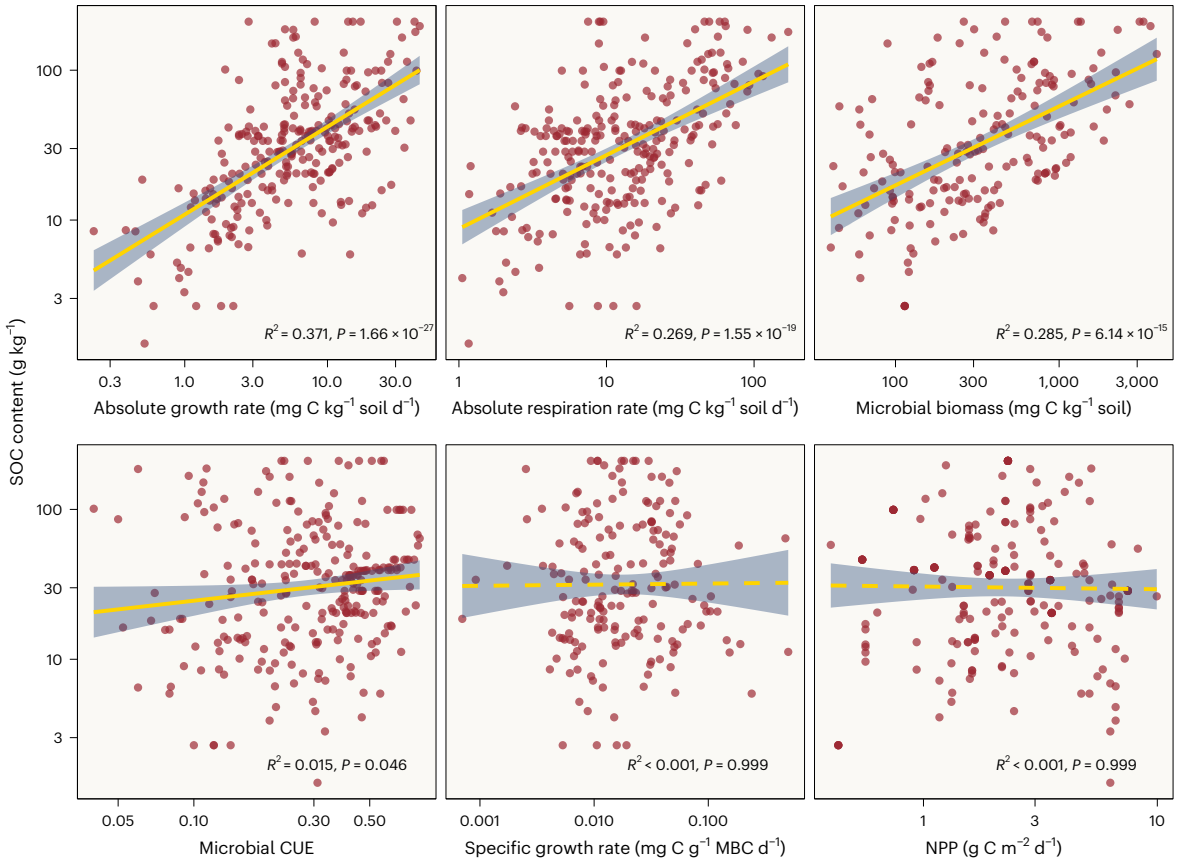

Fig. 2 | Relationships between SOC and microbial or ecosystem properties based on observational data. SOC versus absolute growth rate, absolute respiration rate, microbial biomass, microbial CUE, specific microbial growth rate and NPP. Both axes are log-transformed; linear regression analyses were performed on log-transformed data. The yellow lines represent the regression fits; the solid lines indicate statistically significant relationships ($P < 0.05$), while the dashed lines indicate non-significant relationships ($P > 0.05$). The shaded bands denote the 95% confidence intervals around the regression estimates. All statistical tests were two-sided. MBC, microbial biomass carbon.

ORCHIDEE-MIMICS explicitly represents microbial processes; the others diagnose microbial properties indirectly under steady-state assumptions (Supplementary Fig. 4). The CUE values reported refer to system-level emergent CUE, not the fixed values assigned to the individual decomposition pathways in the model.

Simulations revealed large variability in emergent CUE across models, both in magnitude and spatial distribution (Fig. 4a–e). For example, CUE values in CABLE-CASA were narrowly constrained (0.15–0.25), whereas the other models produced broader ranges. On the other hand, microbial growth rates were more spatially consistent and tightly constrained (Fig. 4f–j). Correlations confirmed this pattern: growth rates were highly consistent across models (ρ = 0.82–0.94, $P < 0.001$), whereas CUE correlations were weaker and sometimes negative (Fig. 4k–m). SOC projections themselves showed moderate agreement across models (ρ = 0.57–0.92) and with the Harmonized World Soil Database (HWSD) (ρ = 0.51–0.59).

Direct regressions indicated that modelled microbial growth rates predicted SOC more strongly than CUE (R^2 = 0.04–0.67 versus 0.02–0.15; Supplementary Fig. 5). To test whether the microbial growth rate provides more information than plant inputs alone, we compared the SOC–growth and SOC–NPP relationships across the four models (Supplementary Figs. 5 and 6). In all models, the microbial growth rate was tightly correlated with NPP (R^2 = 0.883–0.986; Supplementary Fig. 6), reflecting the dominant role of plant inputs in driving the microbial growth rate within models. However, the strength of SOC–growth versus SOC–NPP associations differed among models. In ORCHIDEE-MIMICS, which has explicit microbial-mineral stabilization pathways, SOC was more strongly linked to growth (R^2 = 0.668, $P < 0.001$; Supplementary Fig. 5b) than to NPP (R^2 = 0.491, $P < 0.001$; Supplementary Fig. 6b), indicating that explicit representation of microbial processes partially decouples SOC storage from inputs by incorporating microbial feedback and stabilization mechanisms. On the other hand, in the three models without explicit modelling of soil microbes (ORCHIDEE-CENTURY, CABLE-CASA and JULES-RothC), the SOC–growth and SOC–NPP relationships were very similar, which is consistent with SOC accumulation being largely input-driven. Across all models, CUE showed only weak (R^2 = 0.073–0.190) or negative (R^2 = 0.348–0.467) associations with NPP (Supplementary Fig. 6). Together, these results suggest that the microbial growth rate can capture both the magnitude of inputs and the modifying influence of microbial feedback, whereas CUE does not.

Random forest analysis supported these results (Fig. 3b and Supplementary Fig. 7): the growth rate was the most important microbial predictor of SOC, while CUE showed little explanatory power. Notably, microbial properties outweighed abiotic predictors such as clay content and MAT in all models, suggesting that current formulations overemphasize microbial control relative to physical drivers. Overall, while the microbial growth rate remains a more consistent predictor of SOC than CUE, the models tend to exaggerate microbial influence and underrepresent abiotic controls compared with observations.

SOC-to-NPP ratio observations highlight growth and physical factors whereas models emphasize CUE

To account for variation in carbon inputs, we normalized SOC according to NPP. This ratio (SOC-to-NPP), which represents soil carbon residence time under steady-state conditions, reflects the capacity of soils to

https://doi.org/10.1038/s41559-025-02961-8

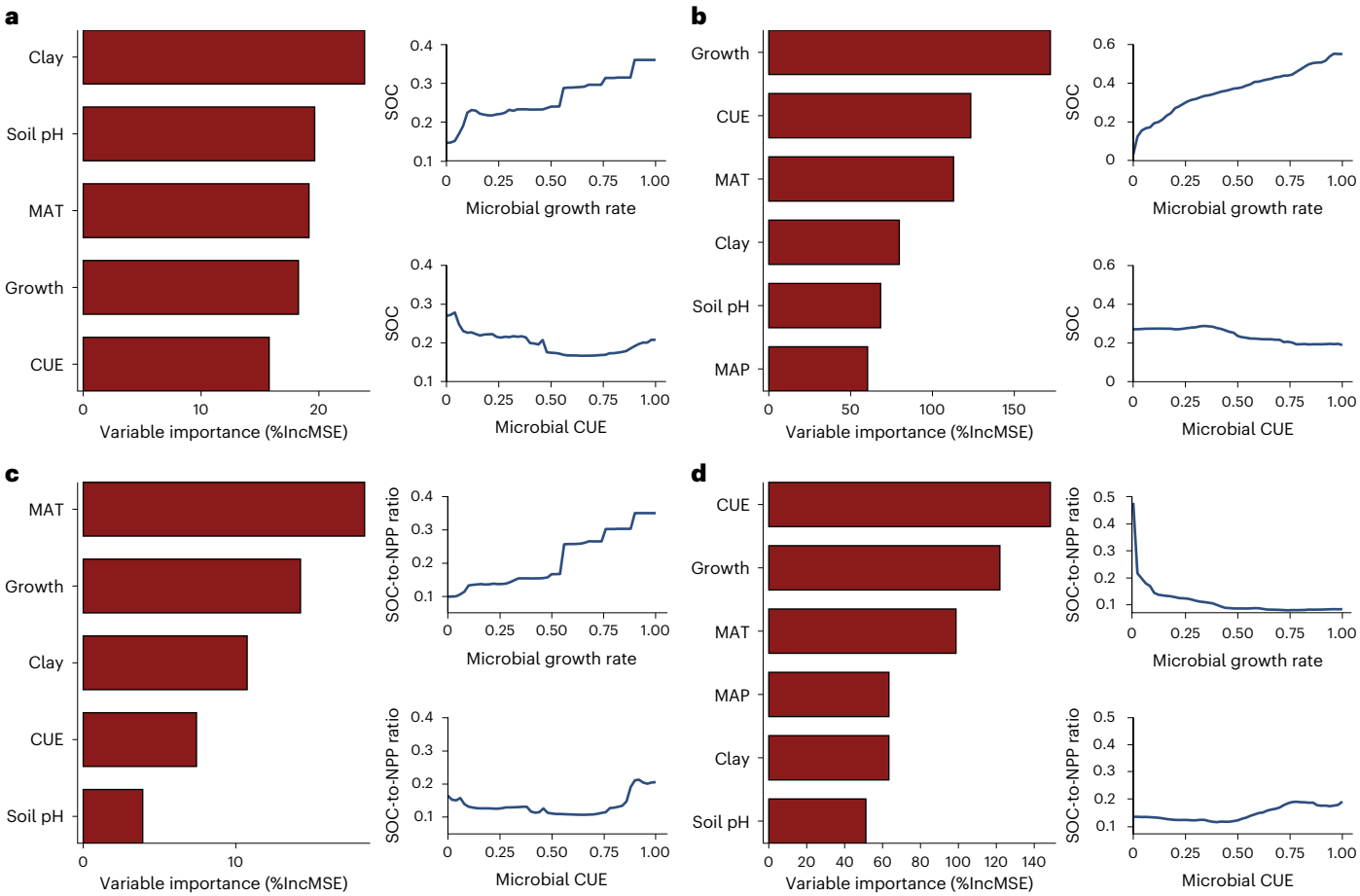

Fig. 3 | Variable importance of microbial and environmental factors for SOC and SOC-to-NPP. a, SOC in the observational data. **b**, SOC across four land surface models. **c**, SOC-to-NPP ratios in the observational data. **d**, SOC-to-NPP ratios across four land surface models. Variable importance was quantified using random forest permutation importance, expressed as the percentage increase in mean squared error (%IncMSE). The partial dependence plots to the right of each panel show the marginal effects of the microbial growth rate (top) and microbial CUE (bottom) on SOC or SOC-to-NPP.

retain plant carbon inputs as SOC. We then used random forest analysis to identify the factors that regulate this ratio. In the observational dataset (using site-level MODIS NPP), microbial absolute growth rate and MAT emerged as the strongest predictors of SOC-to-NPP, whereas CUE had only a minor role (Fig. 3c). In contrast, model simulations showed the opposite pattern: CUE consistently ranked as the dominant predictor of SOC-to-NPP, exceeding microbial growth rate and environmental variables in importance (Fig. 3d). This strong effect of growth at low SOC-to-NPP values reflects model structure: low growth occurs in low-input, low-SOC regimes where SOC-to-NPP is extremely sensitive to small increases in NPP-driven growth. Moreover, across all models, microbial properties generally ranked above abiotic drivers for both SOC and SOC-to-NPP (Fig. 3b,d), whereas in observations, environmental factors such as MAT explained variance comparable to or greater than microbial growth (Fig. 3a,c). Together, the model-imposed coupling of microbial growth to NPP, which produces steep SOC-to-NPP sensitivity under low-input conditions, and the persistent overemphasis of microbial predictors relative to abiotic controls, explain a major part of the model–data mismatch.

We further explored microbial controls under changing inputs using elevated CO_2 simulations in ORCHIDEE-MIMICS and ORCHIDEE-CENTURY. In both models, the absolute change in SOC (ΔSOC) over the 300-year simulation after CO_2 doubling driven by stimulated plant productivity and increased carbon inputs, was primarily explained by changes in microbial growth rate (ΔGrowth), with changes in CUE (ΔCUE) having a secondary role (Supplementary Fig. 8a). To assess how efficiently additional plant inputs were converted into SOC, we normalized ΔSOC according to ΔNPP. This ratio (ΔSOC-to-ΔNPP) represents the sensitivity of SOC to changes in NPP and serves as a diagnostic of retention efficiency. Under this metric, the pattern was reversed: CUE became the strongest predictor of ΔSOC-to-ΔNPP in the models' simulations (Supplementary Fig. 8b).

Together, these results suggest that in models, microbial growth rates are closely tied to NPP and thus govern the magnitude of SOC accumulation, whereas CUE determines how much of the extra inputs due to elevated CO_2 are retained as SOC. This reflects model formulations, where microbial growth largely mirrors spatial and temporal variations in NPP and CUE is the result of coefficients partitioning NPP between respiration and retention in the soil compartments. In contrast, observational data show no strong link between CUE and SOC-to-NPP, implying that current models may oversimplify soil carbon cycling by overemphasizing microbial allocation and underrepresenting other mechanisms important in real ecosystems.

Discussion

By combining global observations with four land surface models, we show that the absolute microbial growth rate is more strongly associated with SOC dynamics than CUE. This stronger association reflects its mechanistic role in linking carbon assimilation to microbial biomass production and necromass formation, which is the key precursor of stable SOC[6,26]. Because the growth rate integrates uptake and allocation processes, it serves as a more direct and quantifiable indicator of

https://doi.org/10.1038/s41559-025-02961-8

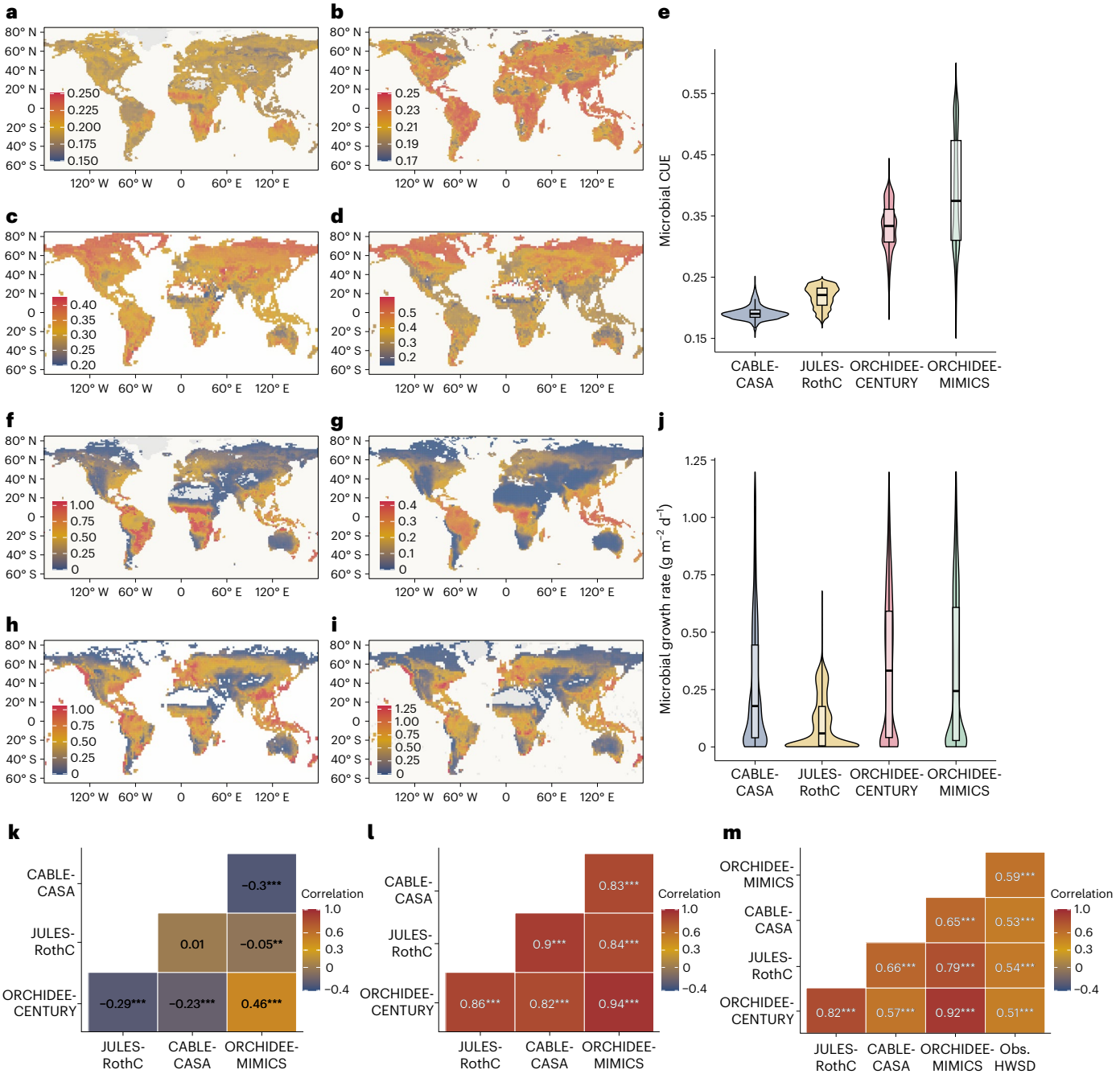

Fig. 4 | Spatial distributions, variability and correlations of microbial properties across four land surface models. a–**e**, Spatial maps and violin plots showing the distribution and variability of microbial CUE simulated by each model. **a**, CABLE-CASA. **b**, JULES-RothC. **c**, ORCHIDEE-CENTURY. **d**, ORCHIDEE-MIMICS. **e**, Microbial CUE. **f**–**j**, Spatial maps and violin plots for the microbial growth rate. **f**, CABLE-CASA. **g**, JULES-RothC. **h**, ORCHIDEE-CENTURY. **i**, ORCHIDEE-MIMICS. **j**, Microbial growth rate. Each violin plot reflects independently simulated grid cells for each model (CABLE-CASA: $n = 7{,}117$; JULES-RothC: $n = 7{,}367$; ORCHIDEE-CENTURY: $n = 4{,}762$; ORCHIDEE-MIMICS: $n = 4{,}666$), which serve as independent spatial units of analysis. The box plots indicate the median (centre line), interquartile range (25th–75th percentiles) and whiskers extending to the most extreme values within 1.5× the interquartile range; outliers beyond this range are omitted for clarity. **k**–**m**, Spearman correlation of spatial patterns, showing model–model correlations for microbial CUE (**k**), model–model correlations for microbial growth rate (**l**) and correlations between simulated SOC and observed SOC from the HWSD database (Obs. HWSD) (**m**). The numerical values denote correlation coefficients; the asterisks indicate the significance level (**$P < 0.01$, ***$P < 0.001$). All correlation tests were two-sided.

microbial contributions to soil carbon cycling than the ratio-based metric of CUE[16,27,34,35]. Notably, the correlation between the absolute microbial growth rate and SOC may partly reflect microbial adjustments in biomass in response to SOC availability because microbial biomass is known to scale with SOC across ecosystems[3]. However, the absolute growth rate is not simply a proxy for biomass. It also integrates the pace of microbial carbon assimilation and allocation, which are processes not captured by biomass alone. This suggests that the absolute microbial growth rate provides mechanistically relevant information for understanding SOC dynamics.

Although many studies reported significant positive relationships between microbial CUE and SOC in both empirical observations and process-based models[12,19,21,31,36], our results suggest that the influence of CUE on SOC is more context-dependent than previously assumed[19,31,36,37].

In our global dataset of 268 observations obtained with the $^{18}O–H_2O$ labelling method (incubation times ≤48 h), CUE showed no significant relationship with SOC. Because this approach is relatively insensitive to incubation duration and includes a pre-incubation step that minimizes wet-up effects, these particular methodological artefacts[37,38] are unlikely to explain the lack of correlation with SOC. Instead, the explanation is more fundamental: CUE is a ratio that describes the partitioning of assimilated carbon between growth and respiration but it does not capture the absolute fluxes of carbon through microbial biomass and necromass[39]. Moreover, measured CUE represents a transient microbial property that fluctuates on hourly to daily timescales, whereas SOC changes over decades to centuries[31]. This temporal mismatch naturally weakens their association[37]. Although microbial growth rate estimates are subject to the same incubation-related limitations as CUE, the relationship between growth rate and SOC is robust and less sensitive to experimental conditions. This is because the microbial growth rate quantifies the magnitude of carbon fluxes and is directly linked to SOC availability and microbial biomass. On the other hand, CUE compounds uncertainties from measurements of both growth and respiration while excluding biomass effects, which weakens its association with SOC in experimental contexts[31,36,37]. These considerations highlight the limitations of relying on ratio-based metrics such as CUE to capture SOC dynamics in empirical evidence[15,40].

Model simulations partially support these conclusions by reproducing the stronger association between microbial growth rate and SOC than between CUE and SOC. However, they also diverge from observations by overemphasizing microbial controls relative to abiotic factors, a pattern that is consistent with Georgiou et al.[41]. In soil carbon models, SOC stocks are the result of input and output carbon fluxes (for example, decomposition), which in turn depend on rate constants that are tuned during model calibration. By contrast, emergent CUE is a by-product of these calibrated fluxes and is not directly constrained in the calibration process. Consequently, even though emergent CUE values differed widely among models, all four models produced similar SOC estimates[42–44] (Fig. 4). This structural feature also explains why, in model simulations, microbial growth rate, as determined by decomposition rates and carbon allocation strategies, shows a stronger correlation with SOC than CUE and is also tightly linked to NPP. The link to NPP is a direct consequence of the equilibrium conditions these models attained; larger NPP implies larger carbon fluxes through all the model pools and thus a higher microbial growth rate. However, we also found important nuances in this coupling among models. In ORCHIDEE-MIMICS, the NPP–growth correlation was weaker (R^2 = 0.88 versus > 0.97 in the other models), reflecting its explicit representation of microbial feedbacks and stabilization processes, such as sorption, aggregation and dissolved losses, which reduce the direct control of NPP on SOC and partly decouple inputs from stocks[45,46]. This agrees with expectations from microbial-explicit models, in which decomposition depends on both substrate and microbial biomass rather than substrate alone[47,48]. Despite this nuance, all models still gave more weight to microbial properties than to abiotic factors, such as clay content and temperature, suggesting that current structures overemphasize microbial controls. Future models should better integrate microbial and abiotic drivers to capture SOC dynamics more realistically[46]. Overall, while the strong growth–SOC link partly reflects model design, the microbial growth rate remains a useful diagnostic that integrates carbon inputs and allocation strategies, providing a benchmark for evaluating model realism.

Despite its central role in carbon cycling, the microbial growth rate is usually treated as an emergent property in soil carbon models—indirectly inferred as the product of CUE and decomposition (or carbon uptake) rate[9,49,50]. This approach limits alignment with empirical evidence. A more process-based strategy is to explicitly simulate microbial carbon uptake and biomass production from measurable traits and environmental drivers[51]. Doing so would reduce structural uncertainty and promote more mechanistically grounded model development[52]. Recent advances in molecular techniques now make such parameterization more feasible. Metagenomic and transcriptomic approaches can provide information on microbial growth potential and realized activity across taxonomic and biogeographical scales[53,54], offering a strong basis for model parameterization.

Our results reveal a clear mismatch between models and observations in the relationships between SOC/NPP and microbial properties. SOC/NPP, which represents soil carbon residence time under steady-state conditions[55,56], shows contrasting controls in the two approaches. In the observational data, SOC/NPP was strongly associated with the absolute microbial growth rate but only weakly with CUE. In contrast, models assigned a dominant role to CUE, especially under elevated CO_2 (ΔSOC/ΔNPP), even though emergent CUE was not a strong predictor of SOC stocks. This means that while CUE contributes little to explaining steady-state SOC, models emphasize its role in determining how efficiently new carbon inputs are retained under changing conditions or management initiatives. This discrepancy probably arises from structural assumptions in current models, where decomposition and substrate availability tightly constrain carbon cycling[48]. Thus, models may overemphasize the role of microbial partitioning while underrepresenting physical stabilization. Therefore, future models should better integrate microbial and abiotic mechanisms to represent SOC dynamics more realistically, particularly under changing environmental conditions or management initiatives (for example, the '4 per mille' initiative[57]).

In conclusion, by integrating global $^{18}O–H_2O$ observations with four land surface models, we demonstrate that the microbial growth rate predicts SOC more consistently than CUE. Observations further reveal that abiotic factors, such as clay content and climate, explain equal or greater variation in SOC, highlighting strong physical constraints over microbial effects. Models capture the stronger role of microbial growth rate relative to CUE for SOC but they tend to overemphasize microbial controls at the expense of abiotic drivers. Together, these findings establish microbial growth rate as a process diagnostic linking models with observations and for rebalancing microbial and abiotic drivers in projections of soil carbon dynamics.

Methods

Observation data collection

We used the microbial growth rate and CUE observations compiled by Hu et al.[16,58], including 268 measurements obtained using the $^{18}O–H_2O$ labelling method. In this approach, microbial growth is quantified by tracking the incorporation of ^{18}O into DNA, which is then converted to gross biomass production (mg C kg^{-1} soil h^{-1}), while microbial respiration is estimated from total CO_2 efflux. Alongside microbial CUE and the growth rate data, associated variables such as MAT, mean annual precipitation (MAP), SOC, incubation temperature and MBC were also extracted. In addition, the NPP for each site was derived from the MODIS data[59] based on the reported latitude and longitude.

Land surface model simulations

We conducted simulations using four land surface models, that is, ORCHIDEE-CENTURY, ORCHIDEE-MIMICS, CABLE-CASA and JULES-RothC, by equilibrating SOC stocks to the boundary conditions of the year 1700. The simulation protocol followed the guidelines of the TRENDY model intercomparison project[60], which standardizes the spin-up procedures for biogeochemical cycles under pre-industrial conditions. Each of the four models incorporates a distinct, widely used soil organic matter (SOM) module: ORCHIDEE-CENTURY[61], ORCHIDEE-MIMICS[62], CABLE-CASA[63] and JULES-RothC[64], respectively. ORCHIDEE-CENTURY and ORCHIDEE-MIMICS share an identical model structure except for their SOM modules, allowing us to isolate the effects of SOM representation on model outputs, an approach not feasible when comparing structurally distinct models.

All model outputs were aggregated to grid-cell averages by combining values across all plant functional types within each grid cell. To reduce interannual variability, we averaged all model outputs

over a 30-year period. Environmental drivers used in each model, including MAT, MAP, soil pH and clay content, were also extracted to assess their influence on spatial variation in SOC and microbial traits. For models that do not provide soil pH internally (for example, ORCHIDEE-CENTURY and JULES-RothC), we supplemented the missing values by extracting the corresponding pH from a global gridded dataset[65] at each cell, thereby ensuring consistent coverage across all models for the combined analyses.

Emergent CUE in land surface models

Among the four land surface models analysed, ORCHIDEE-CENTURY, CABLE-CASA and JULES-RothC do not explicitly simulate microbial biomass pools. Instead, they represent microbial processes implicitly through the partitioning of decomposed carbon into respiration (CO_2 release) and transfer to downstream carbon pools. To approximate microbial CUE in these models, we followed a flux-based approach[37,66,67], calculating the fraction of carbon retained in the receiving pool relative to the total flux from the donor pool. This fraction, representing the portion that was not respired, was used as a proxy for microbial CUE (see conceptual illustration in Supplementary Fig. 4). This flux-based CUE is not a direct microbial trait but rather a proxy inferred from carbon flow partitioning within the model structure. We define this metric as emergent CUE, representing a system-level carbon use efficiency that arises from the balance of carbon fluxes between pools and losses via respiration. Emergent CUE integrates microbial allocation behaviour and model structural assumptions and can be consistently applied across both microbial-explicit models (for example, MIMICS) and microbial-implicit models (for example, CENTURY, CASA, RothC), thereby facilitating comparison of modeled SOC retention and evaluation of microbial controls on soil carbon dynamics.

In cases where multiple upstream carbon fluxes contributed to a receiving pool, we estimated a flux-weighted average CUE as equation (1):

$$\mathrm{CUE}_{\mathrm{avg}} = \frac{\sum_{i=1}^{n} F_i \mathrm{CUE}_i}{\sum_{i=1}^{n} F_i} \quad (1)$$

where F_i is the total carbon flux entering from upstream pool i and CUE_i is the fraction of that flux retained in the receiving pool (that is, not lost as CO_2). In this context, $\mathrm{CUE}_{\mathrm{avg}}$ represents the overall efficiency with which incoming carbon is retained, averaged across all contributing fluxes.

Similarly, the total microbial growth, defined as the sum of retained carbon from all upstream fluxes, was calculated as equation (2):

$$\mathrm{Growth}_{\mathrm{total}} = \sum_{i=1}^{n} F_i \mathrm{CUE}_i \quad (2)$$

CO_2 doubling experiment

To evaluate the response of soil carbon processes to elevated atmospheric CO_2, we conducted an additional experiment using ORCHIDEE-CENTURY and ORCHIDEE-MIMICS. Starting from the previously simulated steady-state SOC conditions, we doubled atmospheric CO_2 concentration and ran the models for an additional 300 years. We then compared SOC stocks, microbial growth rates, and CUE values before and after the CO_2 perturbation, computing the changes in each (ΔSOC, ΔGrowth, ΔCUE). Elevated CO_2 stimulated plant productivity, and consequently carbon inputs to the soil. The magnitude of this stimulation varied spatially, depending on interactions among water availability, temperature, atmospheric CO_2 concentration, and soil nutrient status.

Data analysis

We first examined the value ranges and spatial distributions of microbial CUE and the growth rate as predicted by four land surface models. Pairwise Spearman correlation analyses were conducted to assess spatial consistency among these variables. To ensure comparability, all datasets were resampled to a common spatial resolution of two degrees, corresponding to the coarsest dataset (ORCHIDEE), using a grid-averaging approach before the spatial correlation analysis. Model performance was further evaluated by comparing model-predicted SOC with observed SOC from the HWSD database.

We explored the relationships between microbial properties (microbial growth rate, CUE, microbial biomass and respiration rate) and SOC using univariate linear regression analyses. Additionally, we examined how microbial growth rate and CUE correlated with other microbial properties.

To identify the primary microbial drivers of SOC variation across space and under elevated CO_2, we conducted two sets of random forest regression analyses. For the spatial analysis, we used microbial properties (growth rate and CUE), climate variables and soil properties as predictors, and SOC as the response variable. As the models produced broadly consistent results (Supplementary Fig. 8), this aggregation allowed a unified interpretation across models. Model outputs from the four land surface models were first min–max scaled (0–1 range) and then combined to ensure comparability (Supplementary Fig. 9).

Random forest models were implemented using the randomForest package (v.4.6-12)[68] in R (v.4.3.0), with 500 trees ($n$tree = 500) and the number of variables sampled at each split ($m$try) set to the square root of the number of predictors. Predictor importance was quantified using the percentage increase in mean squared error according to random permutation. Partial dependence plots were used to visualize the marginal effects of the microbial growth rate and CUE on SOC, isolating non-linear and interactive effects while averaging over other predictors.

To assess microbial controls on SOC response to elevated CO_2, we performed a second random forest analysis using simulation outputs from the two ORCHIDEE models. The response variable was the ratio of ΔSOC-to-ΔNPP, which serves as a diagnostic describing how efficiently additional plant carbon inputs (per unit increase in NPP) were converted into SOC. Predictors included baseline microbial growth rate and CUE, climate variables, soil pH and clay content. This analysis identified which microbial trait most strongly influenced SOC changes under elevated CO_2, independent of productivity effects.

All data processing and statistical analyses were conducted in R (v.4.3.0), and all analytical figures were produced using the ggplot2 package (v.3.5.2). The conceptual schematic presented in Fig. 1 was created in Microsoft PowerPoint 2019 and refined in Inkscape (v.1.3.2) using original graphical elements, without incorporating any third-party copyrighted material.

Reporting summary

Further information on research design is available in the Nature Portfolio Reporting Summary linked to this article.

Data availability

The global observational dataset is available via figshare at https://doi.org/10.6084/m9.figshare.30070084.v1 (ref. 58). Simulation outputs from the four land surface models (ORCHIDEE-CENTURY, ORCHIDEE-MIMICS, CABLE-CASA and JULES-RothC) are also available via figshare at https://figshare.com/s/95f8435036d7f6825a53 (ref. 69). All custom R scripts used for data processing, statistical analyses and figure generation are openly available via Zenodo at https://doi.org/10.5281/zenodo.17800780 (ref. 70).

References

1. Janzen, H. H. The soil carbon dilemma: shall we hoard it or use it? *Soil Biol. Biochem.* **38**, 419–424 (2006).
2. Kuzyakov, Y., Ling, N., Pietramellara, G. & Nannipieri, P. Some new grand questions in soil biology and biochemistry. *Soil Biol. Biochem.* **212**, 109996 (2026).

3. Xu, X., Thornton, P. E. & Post, W. M. A global analysis of soil microbial biomass carbon, nitrogen and phosphorus in terrestrial ecosystems. *Glob. Ecol. Biogeogr.* **22**, 737–749 (2013).
4. Angst, G., Mueller, K. E., Nierop, K. G. J. & Simpson, M. J. Plant- or microbial-derived? A review on the molecular composition of stabilized soil organic matter. *Soil Biol. Biochem.* **156**, 108189 (2021).
5. Liang, C., Amelung, W., Lehmann, J. & Kästner, M. Quantitative assessment of microbial necromass contribution to soil organic matter. *Glob. Change Biol.* **25**, 3578–3590 (2019).
6. Camenzind, T., Mason-Jones, K., Mansour, I., Rillig, M. C. & Lehmann, J. Formation of necromass-derived soil organic carbon determined by microbial death pathways. *Nat. Geosci.* **16**, 115–122 (2023).
7. Liang, C., Schimel, J. P. & Jastrow, J. D. The importance of anabolism in microbial control over soil carbon storage. *Nat. Microbiol.* **2**, 17105 (2017).
8. Xiao, K.-Q. et al. Introducing the soil mineral carbon pump. *Nat. Rev. Earth Environ.* **4**, 135–136 (2023).
9. Allison, S. D., Wallenstein, M. D. & Bradford, M. A. Soil-carbon response to warming dependent on microbial physiology. *Nat. Geosci.* **3**, 336–340 (2010).
10. Tang, J. & Riley, W. J. Weaker soil carbon–climate feedbacks resulting from microbial and abiotic interactions. *Nat. Clim. Change* **5**, 56–60 (2015).
11. Walker, T. W. N. et al. Microbial temperature sensitivity and biomass change explain soil carbon loss with warming. *Nat. Clim. Change* **8**, 885–889 (2018).
12. Tao, F. et al. Microbial carbon use efficiency promotes global soil carbon storage. *Nature* **618**, 981–985 (2023).
13. He, X. et al. Model uncertainty obscures major driver of soil carbon. *Nature* **627**, E1–E3 (2024).
14. Xiao, K.-Q. et al. Beyond microbial carbon use efficiency. *Natl Sci. Rev.* **11**, nwae059 (2024).
15. Craig, M. E. et al. Fast-decaying plant litter enhances soil carbon in temperate forests but not through microbial physiological traits. *Nat. Commun.* **13**, 1229 (2022).
16. Hu, J. et al. Microbial carbon use efficiency and growth rates in soil: global patterns and drivers. *Glob. Change Biol.* **31**, e70036 (2025).
17. Liu, M., Lin, H. & Li, J. Are there links between nutrient inputs and the response of microbial carbon use efficiency or soil organic carbon? A meta-analysis. *Soil Biol. Biochem.* **201**, 109656 (2025).
18. Liu, X. et al. Long-term soil warming decreases soil microbial necromass carbon by adversely affecting its production and decomposition. *Glob. Change Biol.* **30**, e17379 (2024).
19. Luo, Z., Ren, J., Manzoni, S. & Fatichi, S. Temperature controls the relation between soil organic carbon and microbial carbon use efficiency. *Glob. Change Biol.* **30**, e17492 (2024).
20. Schroeder, J. et al. The effect of crop diversification and season on microbial carbon use efficiency across a European pedoclimatic gradient. *Eur. J. Soil Sci.* **76**, e70078 (2025).
21. Yang, Y. et al. Unlocking mechanisms for soil organic matter accumulation: carbon use efficiency and microbial necromass as the keys. *Glob. Change Biol.* **31**, e70033 (2025).
22. Zhao, J. et al. Mineral and microbial properties drive the formation of mineral-associated organic matter and its response to increased temperature. *Glob. Change Biol.* **30**, e70004 (2024).
23. Gao, D., Bai, E., Wasner, D. & Hagedorn, F. Global prediction of soil microbial growth rates and carbon use efficiency based on the metabolic theory of ecology. *Soil Biol. Biochem.* **190**, 109315 (2024).
24. García-Palacios, P. et al. Dominance of particulate organic carbon in top mineral soils in cold regions. *Nat. Geosci.* **17**, 145–150 (2024).
25. Varney, R. M. et al. A spatial emergent constraint on the sensitivity of soil carbon turnover to global warming. *Nat. Commun.* **11**, 5544 (2020).
26. Fan, X. et al. Improved model simulation of soil carbon cycling by representing the microbially derived organic carbon pool. *ISME J.* **15**, 2248–2263 (2021).
27. Simon, E. et al. Microbial growth and carbon use efficiency show seasonal responses in a multifactorial climate change experiment. *Commun. Biol.* **3**, 584 (2020).
28. Yin, L. et al. Variation in rhizosphere priming and microbial growth and carbon use efficiency caused by wheat genotypes and temperatures. *Soil Biol. Biochem.* **134**, 54–61 (2019).
29. Zhang, Q. et al. Effect of field warming on soil microbial carbon use efficiency—a meta-analysis. *Soil Biol. Biochem.* **197**, 109531 (2024).
30. Zheng, Q. et al. Growth explains microbial carbon use efficiency across soils differing in land use and geology. *Soil Biol. Biochem.* **128**, 45–55 (2019).
31. Zhou, J., Luo, Y. & Chen, J. Dilemmas in linking microbial carbon use efficiency with soil organic carbon dynamics. *Glob. Change Biol.* **31**, e70047 (2025).
32. Metze, D. et al. Microbial growth under drought is confined to distinct taxa and modified by potential future climate conditions. *Nat. Commun.* **14**, 5895 (2023).
33. Qu, L., Wang, C. & Bai, E. Evaluation of the ^{18}O-H_2O incubation method for measurement of soil microbial carbon use efficiency. *Soil Biol. Biochem.* **145**, 107802 (2020).
34. Wasner, D. et al. Environment and microbiome drive different microbial traits and functions in the macroscale soil organic carbon cycle. *Glob. Change Biol.* **30**, e17465 (2024).
35. Whalen, E. D., Grandy, A. S., Geyer, K. M., Morrison, E. W. & Frey, S. D. Microbial trait multifunctionality drives soil organic matter formation potential. *Nat. Commun.* **15**, 10209 (2024).
36. Fang, L. Multifaceted links between microbial carbon use efficiency and soil organic carbon sequestration. *Glob. Change Biol.* **31**, e70045 (2025).
37. He, X. et al. Emerging multiscale insights on microbial carbon use efficiency in the land carbon cycle. *Nat. Commun.* **15**, 8010 (2024).
38. Geyer, K. M., Dijkstra, P., Sinsabaugh, R. & Frey, S. D. Clarifying the interpretation of carbon use efficiency in soil through methods comparison. *Soil Biol. Biochem.* **128**, 79–88 (2019).
39. Manzoni, S. & Cotrufo, M. F. Mechanisms of soil organic carbon and nitrogen stabilization in mineral-associated organic matter—insights from modeling in phase space. *Biogeosciences* **21**, 4077–4098 (2024).
40. Spohn, M. et al. Soil microbial carbon use efficiency and biomass turnover in a long-term fertilization experiment in a temperate grassland. *Soil Biol. Biochem.* **97**, 168–175 (2016).
41. Georgiou, K. et al. Divergent controls of soil organic carbon between observations and process-based models. *Biogeochemistry* **156**, 5–17 (2021).
42. Dangal, S. R. S. et al. Improving soil carbon estimates by linking conceptual pools against measurable carbon fractions in the DAYCENT model version 4.5. *J. Adv. Model. Earth Syst.* **14**, e2021MS002622 (2022).
43. Goll, D. S. et al. Strong dependence of CO_2 emissions from anthropogenic land cover change on initial land cover and soil carbon parametrization. *Glob. Biogeochem. Cycles* **29**, 1511–1523 (2015).
44. Xu, H., Zhang, T., Luo, Y., Huang, X. & Xue, W. Parameter calibration in global soil carbon models using surrogate-based optimization. *Geosci. Model Dev.* **11**, 3027–3044 (2018).

45. Varney, R. M., Chadburn, S. E., Burke, E. J. & Cox, P. M. Evaluation of soil carbon simulation in CMIP6 Earth system models. *Biogeosciences* **19**, 4671–4704 (2022).
46. Georgiou, K., Abramoff, R. Z., Harte, J., Riley, W. J. & Torn, M. S. Microbial community-level regulation explains soil carbon responses to long-term litter manipulations. *Nat. Commun.* **8**, 1223 (2017).
47. Wutzler, T. & Reichstein, M. Colimitation of decomposition by substrate and decomposers—a comparison of model formulations. *Biogeosciences* **5**, 749–759 (2008).
48. Sulman, B. N. et al. Multiple models and experiments underscore large uncertainty in soil carbon dynamics. *Biogeochemistry* **141**, 109–123 (2018).
49. Abramoff, R. Z. et al. Improved global-scale predictions of soil carbon stocks with Millennial Version 2. *Soil Biol. Biochem.* **164**, 108466 (2022).
50. Wieder, W. R., Grandy, A. S., Kallenbach, C. M. & Bonan, G. B. Integrating microbial physiology and physio-chemical principles in soils with the MIcrobial-MIneral Carbon Stabilization (MIMICS) model. *Biogeosciences* **11**, 3899–3917 (2014).
51. Tang, J. & Riley, W. J. Revising the dynamic energy budget theory with a new reserve mobilization rule and three example applications to bacterial growth. *Soil Biol. Biochem.* **178**, 108954 (2023).
52. Migliavacca, M. et al. The three major axes of terrestrial ecosystem function. *Nature* **598**, 468–472 (2021).
53. Marschmann, G. L. et al. Predictions of rhizosphere microbiome dynamics with a genome-informed and trait-based energy budget model. *Nat. Microbiol.* **9**, 421–433 (2024).
54. Piton, G. et al. Life history strategies of soil bacterial communities across global terrestrial biomes. *Nat. Microbiol.* **8**, 2093–2102 (2023).
55. Wei, N. et al. Evolution of uncertainty in terrestrial carbon storage in earth system models from CMIP5 to CMIP6. *J. Clim.* **35**, 5483–5499 (2022).
56. Carvalhais, N. et al. Global covariation of carbon turnover times with climate in terrestrial ecosystems. *Nature* **514**, 213–217 (2014).
57. Minasny, B. et al. Soil carbon 4 per mille. *Geoderma* **292**, 59–86 (2017).
58. Hu, J. Database of microbial growth rate outweighs carbon use efficiency in shaping soil carbon dynamics. Dataset. *figshare* https://doi.org/10.6084/m9.figshare.30070084.v1 (2025).
59. Running, S. & Zhao, M. MODIS/Terra Net Primary Production Gap-Filled Yearly L4 Global 500m SIN Grid V061. *NASA Land Processes Distributed Active Archive Center* https://doi.org/10.5067/MODIS/MOD17A3HGF.061 (2021).
60. Friedlingstein, P. et al. Global carbon budget 2023. *Earth Syst. Sci. Data* **15**, 5301–5369 (2023).
61. Parton, W. J., Stewart, J. W. B. & Cole, C. V. Dynamics of C, N, P and S in grassland soils: a model. *Biogeochemistry* **5**, 109–131 (1988).
62. Zhang, H. et al. Microbial dynamics and soil physicochemical properties explain large-scale variations in soil organic carbon. *Glob. Change Biol.* **26**, 2668–2685 (2020).
63. Potter, C. S. et al. Terrestrial ecosystem production: a process model based on global satellite and surface data. *Glob. Biogeochem. Cycles* **7**, 811–841 (1993).
64. Coleman, K. & Jenkinson, D. S. in *Evaluation of Soil Organic Matter Models* (eds Powlson, D. S. et al.) 237–246 (Springer, 1996).
65. Hengl, T. et al. SoilGrids250m: global gridded soil information based on machine learning. *PLoS ONE* **12**, e0169748 (2017).
66. Frey, S. D., Lee, J., Melillo, J. M. & Six, J. The temperature response of soil microbial efficiency and its feedback to climate. *Nat. Clim. Change* **3**, 395–398 (2013).
67. Georgiou, K., Koven, C. D., Riley, W. J. & Torn, M. S. Toward improved model structures for analyzing priming: potential pitfalls of using bulk turnover time. *Glob. Change Biol.* **21**, 4298–4302 (2015).
68. Breiman, L., Cutler, A., Liaw, A. & Wiener, M. randomForest: Breiman and Cutlers random forests for classification and regression. R package version 4.7-1.2 https://doi.org/10.32614/CRAN.package.randomForest (2002).
69. Microbial growth better predicts soil carbon than carbon use efficience. *figshare* https://figshare.com/s/95f8435036d7f6825a53 (2025).
70. He, X. Microbial growth rate is a stronger predictor of soil organic carbon than carbon use efficiency. *Zenodo* https://doi.org/10.5281/zenodo.17800781 (2025).

Acknowledgements

We thank Y. Xi and C. Zhou (Laboratoire des Sciences du Climat et de l'Environnement) for their valuable feedback during manuscript preparation and revision. This study was supported by the CALIPSO project funded by Schmidt Sciences. G.M. and D.S.G. acknowledge support from the EJP Soil ICONICA project. E.S. and S.M. were supported by the European Research Council under the European Union's Horizon 2020 Research and Innovation Programme (grant no. 101001608). H.Z. was supported by the National Natural Science Foundation of China (grant no. 41030052). J.H. was supported by the Natural Science Foundation of Sichuan Province (grant no. 2025ZNSFSC1033) and the Postdoctoral Fellowship Program of the China Postdoctoral Science Foundation (grant no. GZB20250584). Support for Y.-P.W. was provided in part by the Terrestrial Ecosystem Research Network, an Australian Government National Collaborative Research Infrastructure Strategy-enabled project.

Author contributions

X.H., G.M. and D.S.G. conceived and designed the study. J.H. provided the observational dataset. S.M., P.C., Y.-P.W., R.Z.A. and E.A. contributed to the initial development of the study concept and discussions. Y.C. and E.B. supplied the data that supported the preliminary exploratory analyses. P.C. and D.S.G. secured the project funding. All authors contributed to the writing, discussion and revision of the paper.

Competing interests

The authors declare no competing interests.

Additional information

Supplementary information The online version contains supplementary material available at https://doi.org/10.1038/s41559-025-02961-8.

Correspondence and requests for materials should be addressed to Junxi Hu or Daniel S. Goll.

Peer review information *Nature Ecology & Evolution* thanks Luiz A. Domeignoz-Horta and the other, anonymous, reviewer(s) for their contribution to the peer review of this work. Peer reviewer reports are available.

[1]Laboratoire des Sciences du Climat et de l'Environnement, IPSL-LSCE, CEA/CNRS/UVSQ/Université Paris Saclay, Orme des Merisiers, Gif sur Yvette, France. [2]College of Forestry, Sichuan Agricultural University, Chengdu, China. [3]Department of Physical Geography and Bolin Centre for Climate Research, Stockholm University, Stockholm, Sweden. [4]Faculty of Environment, Science and Economy, University of Exeter, Exeter, UK. [5]CSIRO Environment, Private Bag 10, Melbourne, Victoria, Australia. [6]Guangdong Provincial Key Laboratory of Applied Botany, South China Botanical Garden, Chinese Academy of Sciences, Guangzhou, China. [7]Institute of Biology, Freie Universität Berlin, Berlin, Germany. [8]Key Laboratory of Geographical Processes and Ecological Security of Changbai Mountains, Ministry of Education, School of Geographical Sciences, Northeast Normal University, Changchun, China. [9]Changchun Normal University, Changchun, China. [10]School of Forest Resources, University of Maine, Orono, MA, USA. [11]Carbon-Water Research Station in Karst Regions of Northern Guangdong, School of Geography and Planning, Sun Yat-Sen University, Guangzhou, China. [12]These authors contributed equally: Xianjin He, Gaëlle Marmasse. ✉e-mail: junxihu@sicau.edu.cn; dsgoll123@gmail.com

nature portfolio

Corresponding author(s): Xianjin He(xianjin.he87@gmail.com)

Last updated by author(s): Dec 2, 2025

Reporting Summary

Nature Portfolio wishes to improve the reproducibility of the work that we publish. This form provides structure for consistency and transparency in reporting. For further information on Nature Portfolio policies, see our Editorial Policies and the Editorial Policy Checklist.

Statistics

For all statistical analyses, confirm that the following items are present in the figure legend, table legend, main text, or Methods section.

n/a	Confirmed	
☐	☒	The exact sample size (*n*) for each experimental group/condition, given as a discrete number and unit of measurement
☐	☒	A statement on whether measurements were taken from distinct samples or whether the same sample was measured repeatedly
☐	☒	The statistical test(s) used AND whether they are one- or two-sided *Only common tests should be described solely by name; describe more complex techniques in the Methods section.*
☐	☒	A description of all covariates tested
☐	☒	A description of any assumptions or corrections, such as tests of normality and adjustment for multiple comparisons
☐	☒	A full description of the statistical parameters including central tendency (e.g. means) or other basic estimates (e.g. regression coefficient) AND variation (e.g. standard deviation) or associated estimates of uncertainty (e.g. confidence intervals)
☐	☒	For null hypothesis testing, the test statistic (e.g. *F*, *t*, *r*) with confidence intervals, effect sizes, degrees of freedom and *P* value noted *Give P values as exact values whenever suitable.*
☒	☐	For Bayesian analysis, information on the choice of priors and Markov chain Monte Carlo settings
☒	☐	For hierarchical and complex designs, identification of the appropriate level for tests and full reporting of outcomes
☒	☐	Estimates of effect sizes (e.g. Cohen's *d*, Pearson's *r*), indicating how they were calculated

Our web collection on statistics for biologists contains articles on many of the points above.

Software and code

Policy information about availability of computer code

Data collection	Microbial growth rate and carbon use efficiency (CUE) data were compiled from 268 paired measurements obtained using the $^{18}O–H_2O$ DNA labeling method, collected at 92 unique natural ecosystem sites worldwide. These data were extracted from previously published datasets and literature sources, representing natural, undisturbed ecosystems. No original field sampling was performed by the authors.
Data analysis	Statistical analyses, including linear regression, Spearman correlation, and random forest regression, were performed using R software (version 4.3.3). The randomForest package (version 4.6-12) was used for machine learning analyses. Custom R scripts developed to process the data and perform analyses are available upon request. Model simulations were conducted following TRENDY project protocols, and data from four land surface models were aggregated and analyzed using standard R functions.

For manuscripts utilizing custom algorithms or software that are central to the research but not yet described in published literature, software must be made available to editors and reviewers. We strongly encourage code deposition in a community repository (e.g. GitHub). See the Nature Portfolio guidelines for submitting code & software for further information.

Data

Policy information about availability of data

All manuscripts must include a data availability statement. This statement should provide the following information, where applicable:

- Accession codes, unique identifiers, or web links for publicly available datasets
- A description of any restrictions on data availability
- For clinical datasets or third party data, please ensure that the statement adheres to our policy

The global observational dataset of microbial growth rate and carbon use efficiency (CUE), along with simulation outputs from four land surface models (ORCHIDEE-CENTURY, ORCHIDEE-MIMICS, CABLE-CASA, and JULES-RothC), are publicly available at Figshare: https://figshare.com/s/95f8435036d7f6825a53. All data used in this study are open access and free to download. There are no restrictions on data availability.

Research involving human participants, their data, or biological material

Policy information about studies with human participants or human data. See also policy information about sex, gender (identity/presentation), and sexual orientation and race, ethnicity and racism.

Reporting on sex and gender	Not applicable. This study does not involve human participants, and no sex or gender data were collected or analyzed.
Reporting on race, ethnicity, or other socially relevant groupings	Not applicable. No race, ethnicity, or other socially relevant groupings are included or analyzed in this study.
Population characteristics	Not applicable. The study does not include any human participants or population characteristics.
Recruitment	Not applicable. No recruitment of human participants was conducted for this study.
Ethics oversight	Not applicable. This study did not involve human subjects or human data and therefore did not require ethical approval.

Note that full information on the approval of the study protocol must also be provided in the manuscript.

Field-specific reporting

Please select the one below that is the best fit for your research. If you are not sure, read the appropriate sections before making your selection.

☐ Life sciences ☐ Behavioural & social sciences ☒ Ecological, evolutionary & environmental sciences

For a reference copy of the document with all sections, see nature.com/documents/nr-reporting-summary-flat.pdf

Ecological, evolutionary & environmental sciences study design

All studies must disclose on these points even when the disclosure is negative.

Study description	This study synthesizes globally distributed measurements of microbial growth rate and carbon use efficiency together with outputs from four land-surface models to evaluate microbial and abiotic controls on soil organic carbon dynamics.
Research sample	The research sample consists of 268 paired observations of microbial growth rate and CUE, collected from natural, undisturbed ecosystems globally. No experimental manipulations were applied to these samples.
Sampling strategy	No new sampling was performed. Observational sites were included based on data availability in published sources, representing a broad range of climatic and edaphic conditions.
Data collection	No primary data were collected by the authors. All observational data were obtained from previously published studies, and model outputs were generated using established TRENDY protocols.
Timing and spatial scale	Observational data span multiple years from 92 global sites. Model simulations were run to equilibrium under pre-industrial conditions and extended under elevated CO_2 for 300 years.
Data exclusions	No data points were excluded from analyses. Missing values in the observational dataset were retained as gaps and not imputed.
Reproducibility	The analyses were conducted with transparent methods using publicly available data and standard modeling frameworks. Four independent land surface models were compared to verify consistency of findings. Model code and analysis scripts are available upon request.
Randomization	Randomization is not applicable as this study synthesizes observational data and model simulations without experimental grouping or allocation.

Blinding	Blinding was not applicable since the study involved data synthesis and computational modeling rather than experimental data acquisition.

Did the study involve field work? ☐ Yes ☒ No

Reporting for specific materials, systems and methods

We require information from authors about some types of materials, experimental systems and methods used in many studies. Here, indicate whether each material, system or method listed is relevant to your study. If you are not sure if a list item applies to your research, read the appropriate section before selecting a response.

Materials & experimental systems

n/a	Involved in the study
☒	☐ Antibodies
☒	☐ Eukaryotic cell lines
☒	☐ Palaeontology and archaeology
☒	☐ Animals and other organisms
☒	☐ Clinical data
☒	☐ Dual use research of concern
☒	☐ Plants

Methods

n/a	Involved in the study
☒	☐ ChIP-seq
☒	☐ Flow cytometry
☒	☐ MRI-based neuroimaging

Plants

Seed stocks	Not applicable.
Novel plant genotypes	Not applicable.
Authentication	Not applicable.